

Reduction of Charging Effects Using Vector Scanning in the Scanning Electron Microscope

J.T.L. THONG, K.W. LEE, W.K. WONG

Centre for Integrated Circuit Failure Analysis and Reliability (CICFAR), Faculty of Engineering, National University of Singapore, Singapore

Summary: We describe a vector scanning system to reduce charging effects during scanning electron microscope (SEM) imaging. The vector scan technique exploits the intrinsic charge decay mechanism of the specimen to improve imaging conditions. We compare SEM images obtained by conventional raster scanning versus vector scanning to demonstrate that vector scanning successfully reduces specimen-charging artifacts.

Key words: raster scan, scanning electron microscopy, specimen charging, vector scanning

PACS: 07.78.+s, 41.75.Fr, 61.16.-d

Introduction

Specimen charging is a perennial problem when specimens with insulating materials are examined in the scanning electron microscope (SEM). Various methods are available to alleviate charging problems, including notably low-voltage operation (Pawley 1984), specimen coating, and charge neutralization by gas ionization (Moncrieff *et al.* 1978), which is the principle underlying low-vacuum or environmental SEMs. Other methodologies aim to control the charge on the specimen through limiting exposure or selective charge deposition (Wong *et al.* 1995). No single technique is able to address the plethora of specimen charging phenomena due to the complexity of physical interactions with real-life specimens and the dynamic nature of charging (Wong *et al.* 1997). In this paper, we propose the

use of vector scanning to reduce charging artifacts for certain classes of insulating specimens. The technique can be applied to any type of SEM and, indeed, to any charged-particle scanning instrument.

Scanning Methodology

It is well known that imaging at television rates reduces charging artifacts when compared with slow-scan modes of operation (Welter and McKee 1972), and hence, during image acquisition, frame averaging as opposed to line averaging is the preferred method for noise reduction. There are several reasons for this. At slow scan rates, the dwell time of the beam at any point in the scan field is longer, which results in greater discrepancy in the charging states between adjacent or nearby image pixels. Under dynamic charging conditions at high beam energies, this may result in significant beam deflection by lateral surface fields that build up, a condition that is manifested as image smearing between lines. At faster scan rates, the effect is still present, but depending on the scan rate the entire image may appear to drift slowly instead.

Another consequence of slow scan rates is the higher rate of charge deposition while the beam is stationed over a point. The initial rate of charge leakage is invariably smaller than the deposition rate, which means a net buildup of charge in the insulator until either steady-state conditions are achieved or breakdown occurs. The former is attained in the case of positive charging (beam energies below the second crossover), whereas the latter is likely if high-beam energies are used.

In the case of negative charging on a perfectly insulating specimen, the surface potential stabilizes at a potential representing the difference between the beam energy and the second crossover. If the electric field at the specimen surface exceeds the material breakdown field, surface breakdown occurs, initiated at weak points or where the breakdown field is first exceeded as charge is deposited, resulting in a secondary electron (SE) image that looks like a “lightning storm.” Under less severe charging conditions, individual Malter discharge streaks can be observed in the SE image (Shaffner and Hearle 1976). On a “good” insulator with low leakage rates, a slow scan may result in multiple discharges over a single frame, whereas at higher

This work is supported by an NSTB grant NSTB/17/2/3.

Address for reprints:

John T. L. Thong
Centre for Integrated Circuit Failure Analysis and Reliability
(CICFAR)
Faculty of Engineering
National University of Singapore
10 Kent Ridge Crescent
Singapore 119260
e-mail: elettl@nus.edu.sg

scan rates a discharge may occur only once every few frames, which may permit the acquisition of a discharge-free image in between.

For insulators with finite leakage, the incidence of discharge will depend on the amount of charge deposited at any point. At high scan rates, the deposited charge density at and around an irradiated point is less, and by the time the beam returns to the same point after one frame, some of the charge would have dispersed by one mechanism or another. Charge motion is beneficial since conduction helps to neutralize or compensate the excessive charges accumulated on the surface or inside the nonconductive specimen and thus helps to reduce the electric field in its neighborhood. Under such circumstances, it is possible that the sample breaks down at slow scan rates, but not at scan rates above a certain threshold.

In a conventional raster scan pattern, the beam is deflected continuously in the line direction. The charge density in the immediate vicinity of a specific point then consists of contributions from the beam traversing the point along the line direction, as well as contributions from the corresponding point on the line scans above and below the current line. For example, consider a 1000×1000 pixel scan field, with a simple raster frame completed in 1s yielding a pixel dwell time of 1 μ s, and a line time of 1ms. If we consider the immediate eight pixels surrounding any one pixel, this cluster of nine pixels would have accumulated charge at times of -0.999 ms, -1.000 ms, -1.001 ms, -0.001 ms, 0 ms, 0.001ms, 0.999 ms, 1.000 ms, and 1.001 ms relative to the central pixel.

In contrast, if consecutive pixels in the scan are placed far apart, then the same cluster of pixels could have charge contributions spread out over a much longer period of time (up to 1/9 s apart) during the formation of a complete scan field. This would permit the charge at each pixel to dissipate over a longer period and thereby reduce the charge density in the pixel cluster. This simple strategy of modifying the scan pattern such that average distance between consecutive points is maximized can be effective in reducing imaging artifacts due to charging. On specimens with inhomogeneous surface conductivity, even if the localized charges dissipate at different rates, the distribution of charge deposition will at least alleviate specific charge-induced contrast observed in some insulators.

The easiest way to obtain the above-mentioned scan pattern is to use a pseudo-random number generator algorithm to generate a two-dimensional (2-D) scan table. However, a direct mapping of the random number to an array coordinate is not appropriate since the pseudo-random number generation algorithm may yield consecutive scan points that are adjacent to each other. The number of iterations required to build a complete scan table is often difficult to predict, and in some cases the same pixel is visited a few times, although it is possible to eliminate coordinates that had already been chosen. Moreover, a large array allocation to store the scan coordinates is required and this can result in considerable memory usage especially for image sizes

greater than 512×512 pixels. However, the most significant drawback of using pseudo-random coordinates is the unpredictable sequence of charge build-up that can result in erratic beam landing errors (Thong *et al.* 2001).

The algorithm chosen in this work uses the equation:

$$p_{n+1} = p_n + IF \quad (1)$$

where IF is the interlace factor, p_n is the location of the current pixel, and p_{n+1} is that of the following pixel. With this algorithm, the 2-D image matrix is mapped to a one-dimensional (1-D) image strip. The first point of the image strip is the origin (0,0) of the image plane. A specified value of IF is then used to calculate the location of next point. Hence IF is also defined as the number of pixels to skip from the present point to the next point. After the first parse of the 1-D array, the algorithm loops back to the beginning of the array and runs iteratively until all the pixels have been visited once. The resultant 1-D scan sequence is then remapped back to the 2-D plane to form the final scan pattern that is used for the vector scan. Figure 1 illustrates the scan sequence generation for a 3×3 matrix interlaced vector scan.

However, the determination of a suitable IF value to minimize the local charge density is not a straightforward task since larger values of IF may not necessarily produce the best result. For example, some IF values may generate scan sequences that have consecutive scan points that are immediately adjacent to one another in both space and time. In other cases, certain IF values may not be able to generate a complete scan table for the image matrix. For valid values of IF , the distance between two consecutive points in the scan field will vary from point to point. It is a formidable computational task to calculate the distance between consecutive pixels using every possible IF for a particular image size, even for a regular SEM image of 512×512 pixels.

At the present time, only a few selected values of IF have been studied. To provide a figure of merit for a given value of IF , the mean and its standard deviation of the absolute distance between all consecutive coordinates are com-

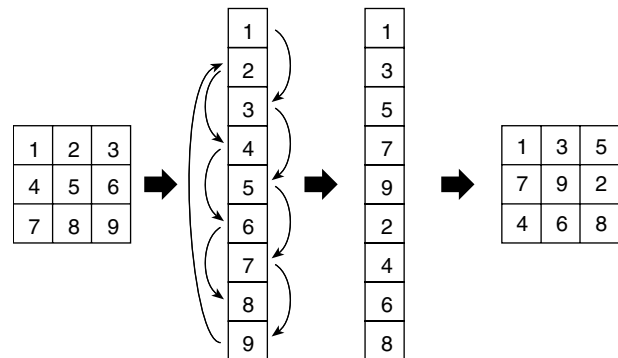


FIG. 1 Interlaced vector scan table generation for a 3×3 image matrix with an IF of 2.

puted. However, the average radial distance between the coordinates and its first consecutive pixel may not necessarily be a good criterion for an optimal scan pattern. One may encounter situations where the second or third consecutive scan coordinates may turn out to be nearer to the reference point compared with its first consecutive pixel. The reason for such a consideration becomes evident particularly for insulators—they dissipate charge relatively slowly so that the excess charge buildup may last for the duration of a few scan points. Hence, the average radial distances d_1 , d_2 , and d_3 are computed for all coordinates corresponding to the separation between the reference point and its first, second, and third consecutive points for a 512×512 image, as shown in Table I. Note that for an IF of 1, corresponding to a conventional raster scan, $d_1 \cong 2.0$ rather than 1 since the scan retraces at the end of every row, adding a distance of around 512 pixels to the start of the next row. The values of d_1 – d_3 values can be readily computed, of which a selection for different IF is shown in Table I. While the parameters d_1 – d_3 provide easily computed values, at best they only provide indicators of IF values to avoid, that is, those that result in close proximity in space and time. The nature of charge buildup on the insulator surface and the manner in which the primary beam is deflected by surface charge requires much more complicated analysis through computer simulation (Thong *et al.* 2001). An IF of 7777 was experimentally found to work well and was selected for all vector scan images described below, unless otherwise stated.

The proposed vector scan technique is not without its difficulties. Specifically, for successful implementation, the deflection system must be capable of settling within a fraction of the pixel dwell time. Typical SEM deflection systems have transient response speeds of around 5–10 μs , which are quite adequate for raster scan deflections. For vector scanning, the implication of the slow deflection speed is that the pixel dwell time can be no faster than the settling time of the deflection system, which would restrict the technique to low frame rates. However, it is possible to reduce the settling time of SEM deflections significantly by modifying the response characteristics of the deflection driver electronics using pre-emphasis techniques—0.5 μs settling times can be readily achieved (Lee and Thong 1999).

TABLE I Distance between a pixel and its first (d_1), second (d_2), and third (d_3) consecutive pixel averaged for all possible coordinates of a 512×512 image for different interlace factors IF

IF	d_1 (pixels)	d_2 (pixels)	d_3 (pixels)
1	2.0	4.0	6.0
3	6.0	11.9	17.7
13	25.4	49.4	72.1
33	61.8	115.0	159.8
577	114.4	195.5	243.6
5555	140.0	230.5	273.9
7777	169.3	260.7	279.9

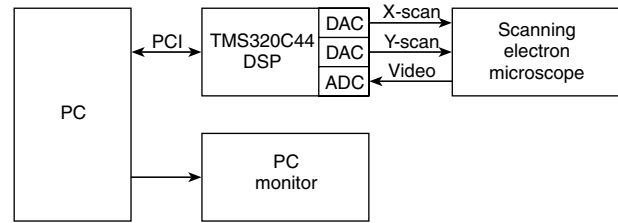


FIG. 2 Block diagram of the overall system. PC=personal computer, DSP=digital signal processor, DAC=digital-to-analog converter, ADC=analog-to-digital converter.

System Implementation

The SEMs used in this work are a Hitachi S-4100 cold field emission (FE) instrument (Hitachi Scientific Instruments, Mountain View, Calif., USA), a Philips XL30 FEG SEM, and a Philips XL30 FEG ESEM (FEI Philips, Peabody, Mass., USA). Figure 2 shows the overall schematic diagram of the system. A TMS320C44 32-bit floating-point digital signal processor (DSP) card plugged into the 32-bit PCI slot of a Pentium personal computer (PC) (Intel Corporation, Santa Clara, Calif., USA) is used to capture the SEM image of the specimen. An independent DSP-based system is chosen to be the platform for implementation to reduce the overheads incurred by the PC when servicing the standard Windows routines. In order to capture the image, the system must synchronize the SE signal acquisition with the SEM scanning. Hence, the DSP card also controls the scanning pattern and speed through two 16-bit digital-to-analog converters (DACs). The maximum deflection speed of the system is limited by the bandwidth of the DACs (~ 200 kHz) and also the dynamic response of the SEM deflection system; however, the latter can be significantly improved by pre-emphasising the deflection signal to reduce the deflection settling time. The vector scan sequences for the x and y coordinates for 256×256 or 512×512 images are pregenerated and stored in the form of two lookup tables (LUTs). The analog video signal from the detector is then digitized with a 16-bit analog-to-digital converter (ADC), which is scaled to 256 gray levels before it is displayed as an image in a client window in a Windows environment.

The image formed immediately after the first few passes through the scan table is very minimal, with barely recognizable features, as shown in Figure 3(a). As more pixels are acquired and filled in, more features can be observed as illustrated in Figure 3(b) and (c). Figure 3(d) shows the image obtained using vector scanning after a single frame has been completely acquired.

Results

The proposed vector scan algorithm has been tested on a wide variety of nonconductive specimens. The results

show that the algorithm performs well, produces good quality images, and is able to reduce charging artifacts in most cases. All the 512×512 pixel images are acquired at a frame time of 13 s. For comparison purposes, conventional raster scanning is simulated by using an interlace factor IF of 1, all other conditions remaining the same.

Optical Fiber

The charging artifact that has been associated with raster scanning is the so-called raster fault. The micrograph in Figure 4(a) shows a classic image of raster faults obtained at a high beam voltage of 30 kV. Vector scanning has effectively eliminated the raster-fault artifact as demonstrated in Figure 4(b); the diagonal bands observed in the image are due to periodic charging-induced beam deflection beating with the scan sequence, which is regular due to the man-

ner in which the coordinates are generated. Note that working at such a high acceleration voltage would often cause radiation damage to nonconductive specimens—in this case, the strong charging due to the injection of high-energy electrons resulted in subsurface charging in the sample even in the vector scanned image.

Photoresist Patterns

The inspection of photoresist patterns on silicon wafers in the SEM plays an important role in the integrated circuit (IC) manufacturing industry. Since polymeric photoresists are electrically insulating, the sample is either coated with a thin layer of gold, or more commonly, the resist sample is viewed at low-beam voltage to reduce charging of the sample by the incident electron beam during SEM inspection or failure analysis.

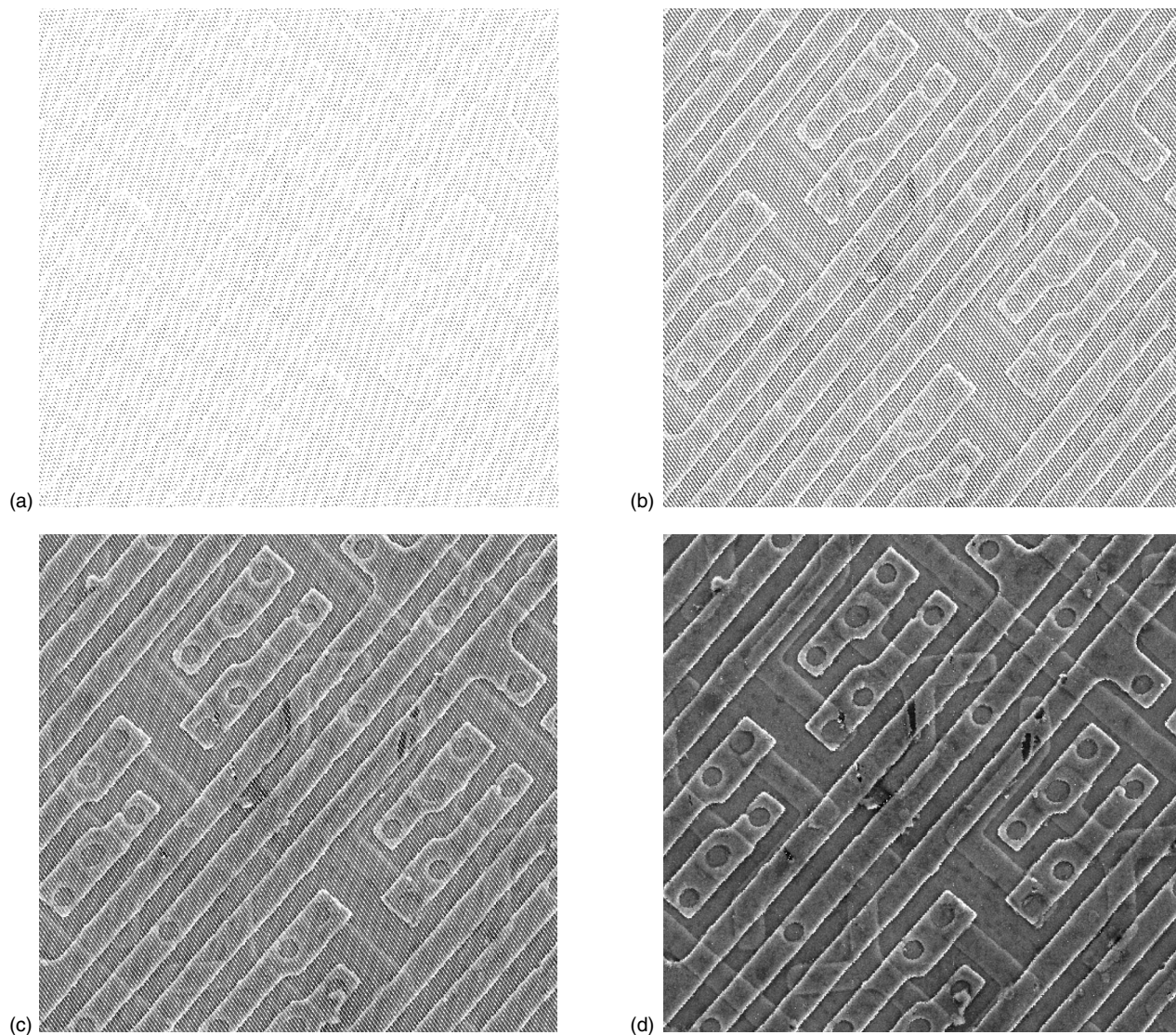
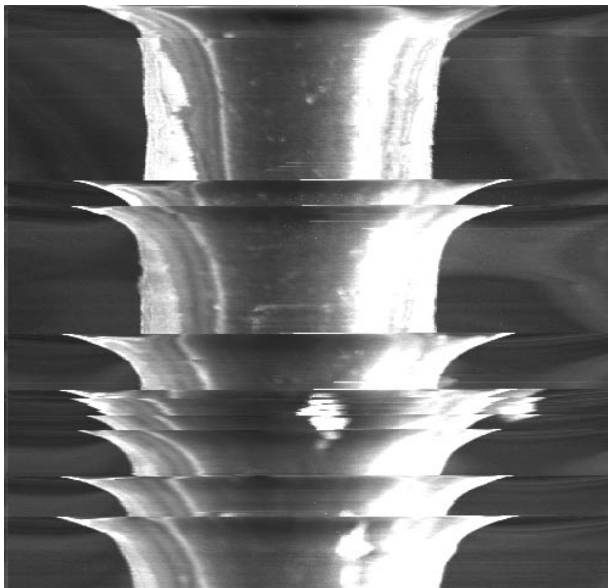


FIG. 3 Scanning electron microscope images obtained at different stages of acquisition, with the time sequence (a)–(d); (d) shows the complete image. Note that the image array is set to full white at the start of acquisition.

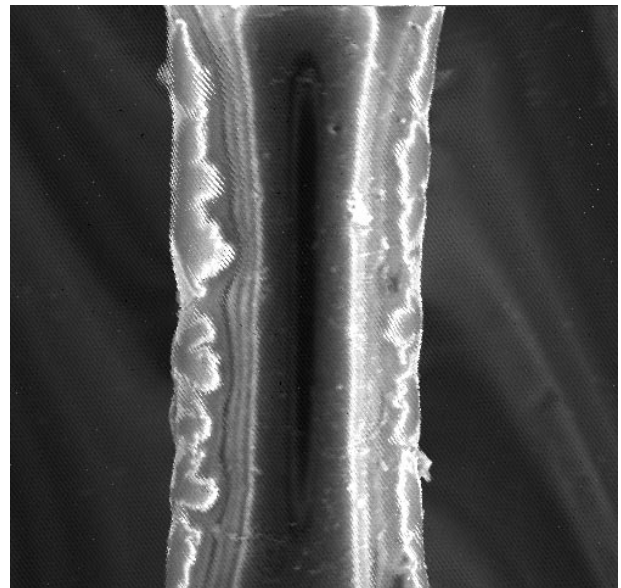
Figure 5(a) and (b) shows the SE images of an uncoated photoresist pattern obtained using raster and vector scans, respectively. The beam voltage used is 2 kV which is slightly above the second crossover of the bulk photoresist. It is apparent from the characteristically bright contrast that the conventional raster scan has resulted in a pattern of negative charge accumulation on the resist. A clearer image of the resist is obtained using the vector scan due to the lower local charge density at any instance in time which allows a degree of charge dissipation.

Defect Analysis

A comprehensive defect analysis is essential in IC manufacturing to improve yield and reliability. Hence, the identification and classification of defects by their features are important for analysis. The SEM is a useful tool for applications that call for resolutions that cannot be attained by optical methods. Figure 6(a) and (b) shows the micrographs of a particle on a photoresist line pattern, using raster and vector scans, respectively. The SE yield enhancement due

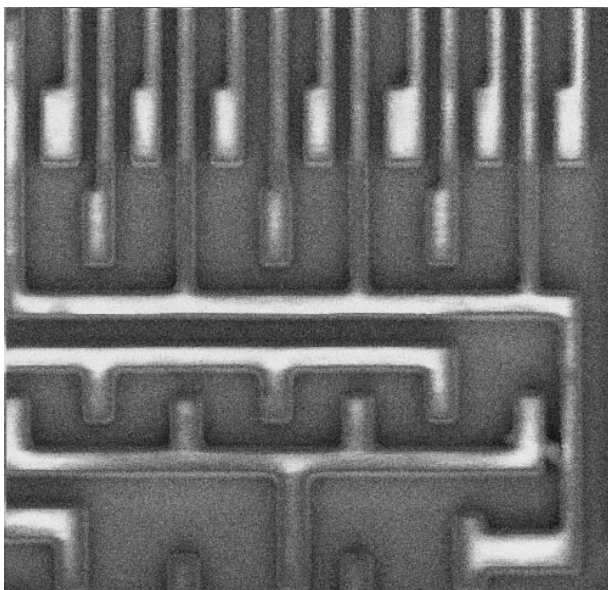


(a)

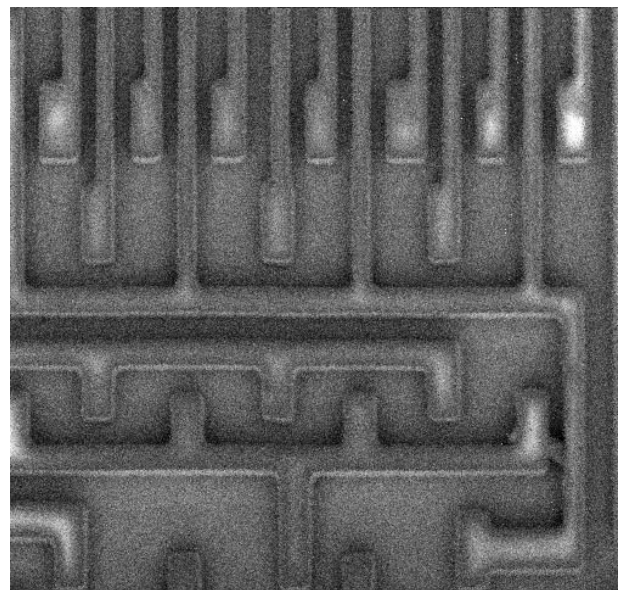


(b)

FIG. 4 Optical fiber imaged at 30 kV using (a) raster scan and (b) vector scan. Horizontal field width = 1 mm.



(a)



(b)

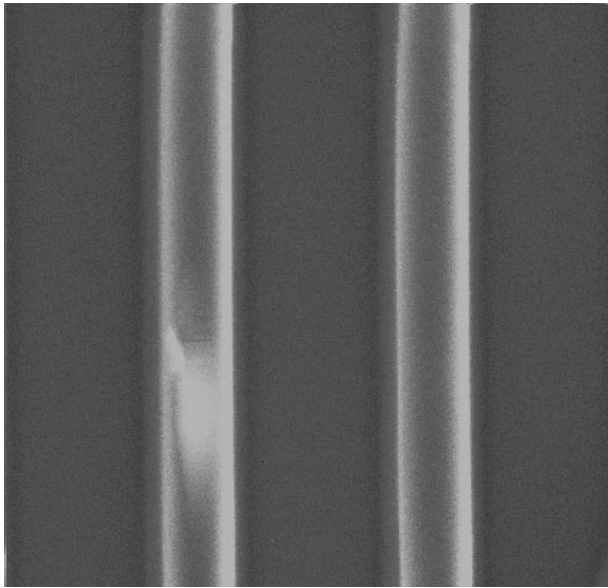
FIG. 5 Photoresist pattern on silicon substrate imaged at 2 kV using (a) raster scan and (b) vector scan. Horizontal field width = 45 μm .

to the defect may be interpreted as accumulation of negative charge on the resist surface. By using the vector scan, the excessive negative charge on the particle is allowed to dissipate away, as shown in Figure 6(b). The contrast around the particle is reduced, allowing better defect analysis.

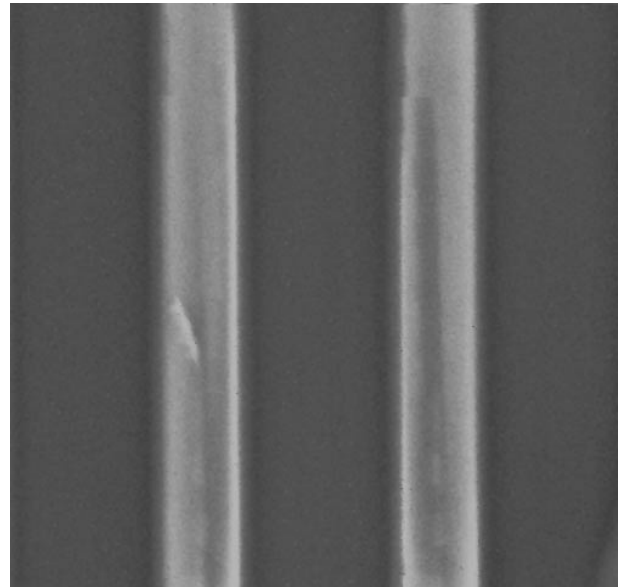
Integrated Circuit Inspection

While gold coating on insulating specimens is often used to render an otherwise insulating surface con-

ductive, it does not eliminate charge completely unless the metal film is fairly thick. With thin films, subsurface charging can result in the deterioration of image quality. An example is shown in Figure 7(a), which is a raster-scan image of a gold-coated passivated IC sample. The charging artifact manifests itself as a defocused image and occasional contrast streaks. These charging artifacts are eliminated when the image is acquired using the vector scan, as shown in Figure 7(b).

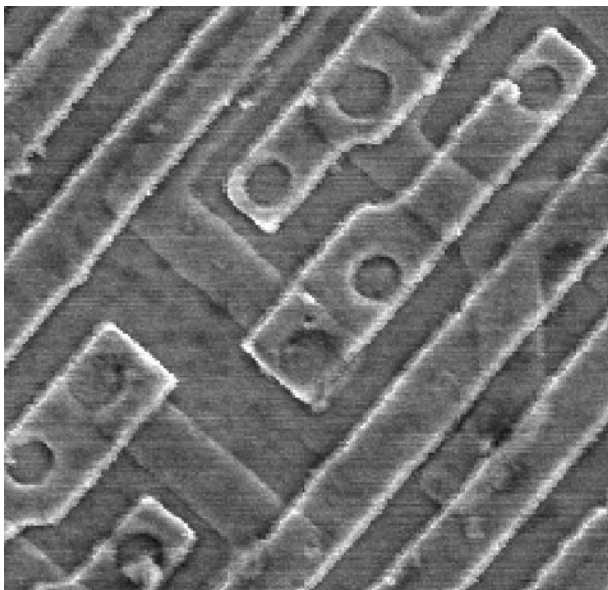


(a)

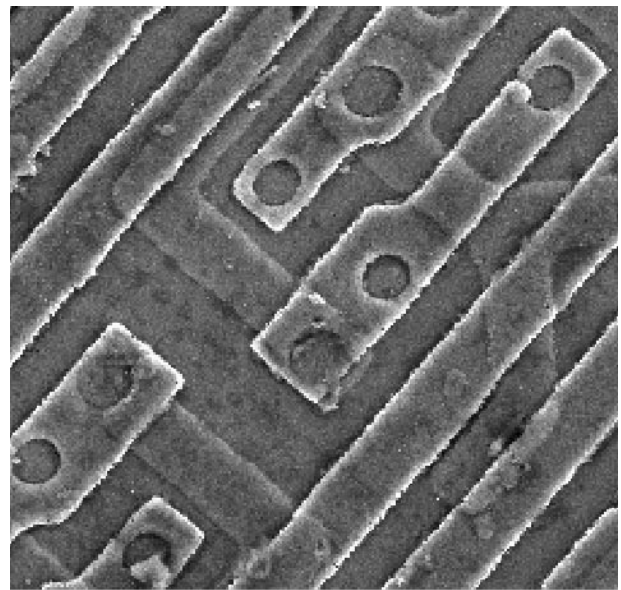


(b)

FIG. 6 Particle on photoresist line pattern imaged at 900 V using (a) raster scan and (b) vector scan. Horizontal field width = 10 μm .



(a)

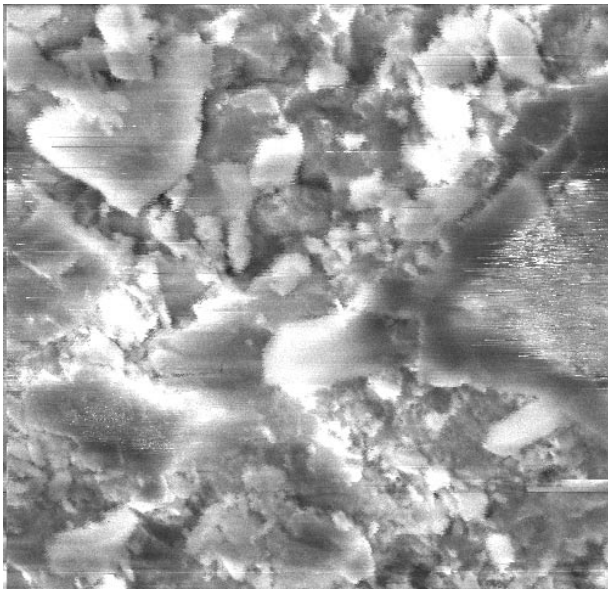


(b)

FIG. 7 Gold-coated passivated integrated circuit sample imaged at 10 kV using (a) raster scan and (b) vector scan. Image resolution is 256 \times 256 pixels. Horizontal field width = 45 μm .

Ceramic Sample

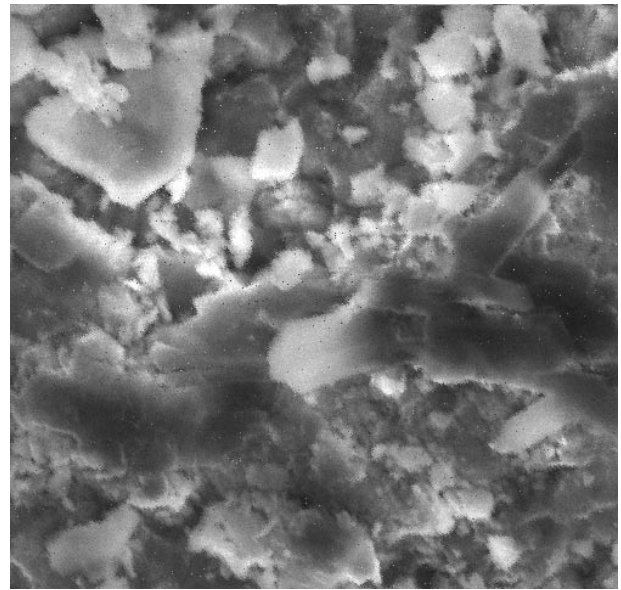
Figure 8(a) shows a typical image of a ceramic with small topographical contrasts obscured by a large contrast component that is due to charging. Adjusting the analog or digital display cannot reduce the masking by the charging artifacts. The insulating nature of the ceramic also produces charging streaks and random charge emissions from its surface which manifest themselves as bright dots and patches. The subtle topographical features are enhanced using the vector scanning method (Fig. 8[b]).



(a)

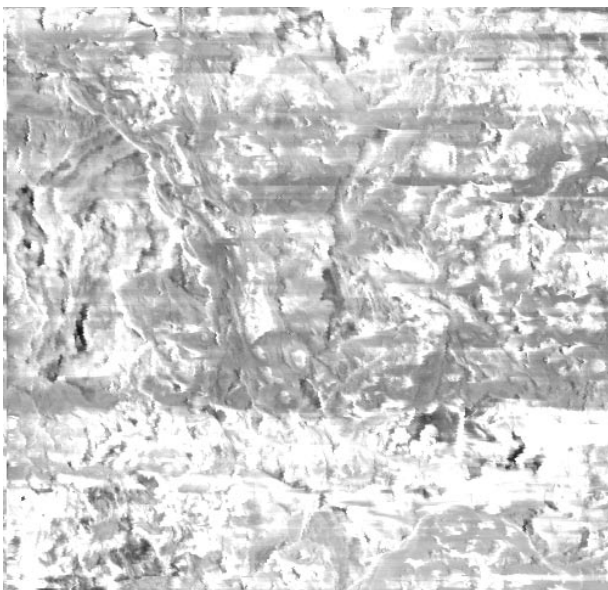
Rock Sample

Figure 9(a) illustrates the bulk charging effect from a rock specimen. Bulk charging contributes a major contrast component of the image and thus masks most of the high-resolution topographical contrasts. This type of specimen is difficult to image in a conventional SEM. The high contrast from the sample saturates the video signal, the contrast and brightness levels of the video system are difficult to adjust, and the image acquired using the raster scan is contaminated with charging streaks. Figure 9(b) shows

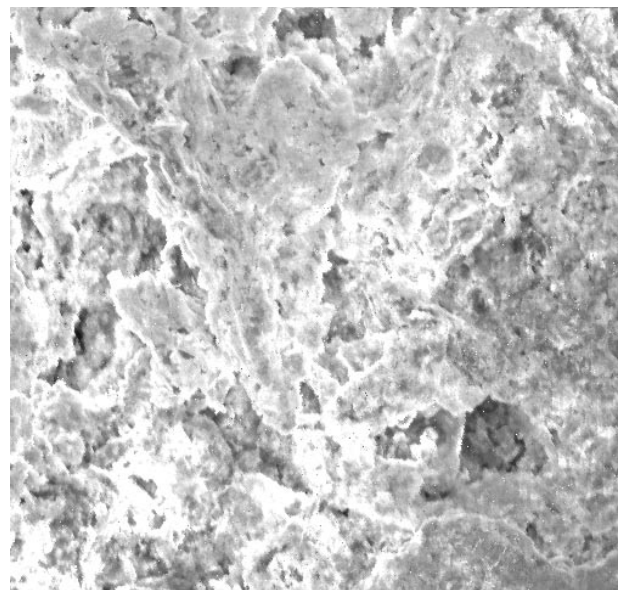


(b)

FIG. 8 Ceramic sample imaged at 15 kV using (a) raster scan and (b) vector scan. Horizontal field width = 80 μm .

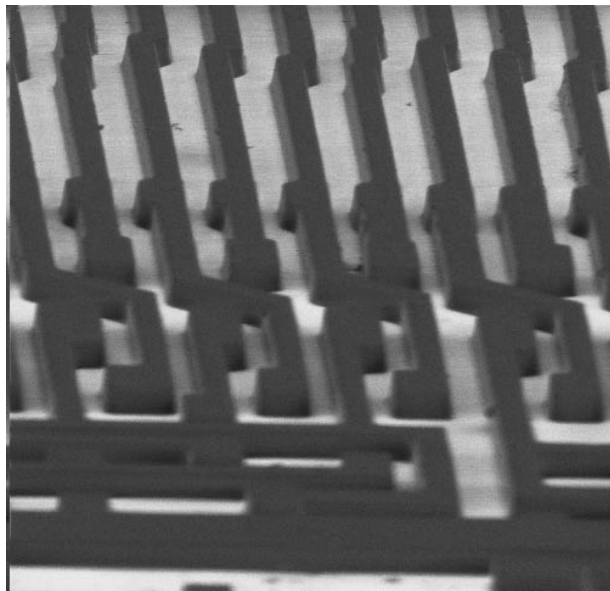


(a)

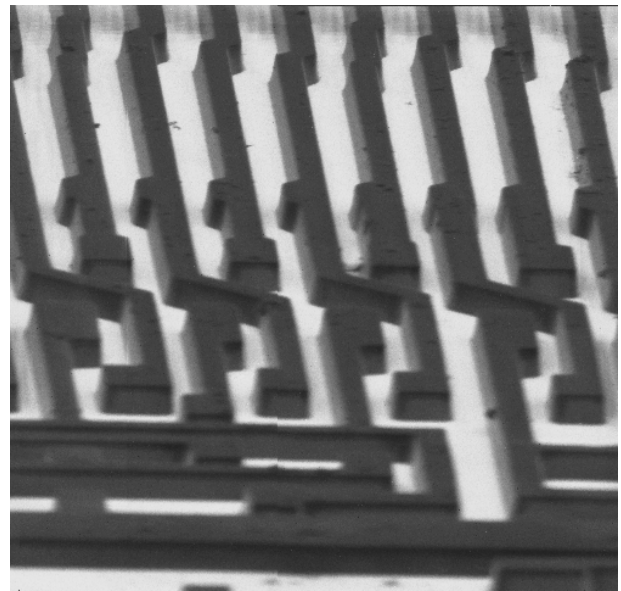


(b)

FIG. 9 Rock sample imaged at 5 kV using (a) raster scan and (b) vector scan. Horizontal field width = 320 μm .



(a)



(b)

FIG. 10 Positive charging of photoresist pattern on silicon substrate imaged at 900 V using (a) raster scan and (b) vector scan. Horizontal field width = 40 μm .

that vector scanning reduces these artifacts and produces a good quality image with clear topographical features.

Positively Charged Resist

The earlier examples demonstrate the reduction of negative charging effects. The effects of positive charging are important for low-voltage SEM operation since positive specimen charging would typically result in a loss in SE signal as low-energy SEs are prevented from leaving the sample by local electric fields (Postek *et al.* 1989). Figure 10(a) shows the image of a positively charged resist pattern obtained with a beam voltage 900 V using raster scanning. Due to the narrow gaps in the resist pattern, part of the SE signal between the lines is suppressed by neighboring positively charged structures of greater relief, giving rise to a shadowing effect. Although changing the scanning pattern does not affect the positive charging state of the surface as much as it does with negative charging—the surface potential stabilizes rapidly under positive charging—the vector scanning method nonetheless reduces the shadowing effect, as shown in Figure 10(b).

Conclusion

In this paper, the performance of vector scanning is evaluated using a wide variety of nonconductive samples. Comparisons between micrographs obtained using conventional raster scanning and vector scanning demonstrate that, in most cases, vector scanning is capable of reducing charging artifacts. Vector scanning is particularly effective in reducing negative charging, artifacts due to positive

charging, and other artifacts such as charging streaks and raster faults.

Acknowledgments

The authors would like to thank Mrs. C.M. Ho, and Mr. K.S. Ng for their kind assistance rendered during this work.

References

- Lee KW, Thong JTL: Improving the speed of scanning electron microscope deflection systems. *Meas Sci Technol* 10, 1070–1074 (1999)
- Moncrieff DA, Robinson VNE, Harris LB: Charge neutralization of insulating surfaces in the SEM by gas ionization. *J Appl Phys D* 11, 2315–2325 (1978)
- Pawley JB: Low voltage scanning electron microscopy. *J Microsc* 136, 54–68 (1984)
- Postek MT, Keery WJ, Larrabee RD: Specimen biasing to enhance or suppress secondary electron emission from charging specimens at low voltages. *Scanning* 11, 111–121 (1989)
- Shaffner TJ, JWS Hearle: Recent advances in understanding specimen charging. *Scan Electron Microsc* 1976/I, 61–70 (1976)
- Thong JTL, WK Wong, Zainal A: Effect of pseudo-random scan parameters on negative specimen charging and beam landing errors in the scanning electron microscope. *Proc. Scanning 2001. Scanning* 23, 113–114 (2001)
- Welter LM, McKee AN: Observations on uncoated, nonconducting or thermally sensitive specimens using a fast scanning field emission source SEM. *Scan Electron Microsc* 1972/I, 161–168 (1972)
- Wong WK, Phang JCH, Thong JTL: Charge control using pulsed scanning electron microscopy. *Scanning* 17, 312–315 (1995)
- Wong WK, Thong JTL, Phang JCH: Charging identification and compensation in the scanning electron microscope. *Proc. 6th IPFA*, 97–102 (1997)